

Experimental evaluation of interfacial adhesion strength of cold sprayed Ti-6Al-4V thick coatings using an adhesive-free test method

Dibakor Bourah, Ben Robinson, Tyler London, Huan Wu, Heidi de Villiers-Lovelock, Philip McNutt, Matthew Doré, and Xiang Zhang

Author post-print (accepted) deposited by Coventry University's Repository

Original citation & hyperlink:

Boruah, Dibakor, et al. "Experimental evaluation of interfacial adhesion strength of cold sprayed Ti-6Al-4V thick coatings using an adhesive-free test method." *Surface and Coatings Technology* (2019): 125130.

<https://dx.doi.org/10.1016/j.surfcoat.2019.125130>

ISSN 0257-8972

Publisher: Elsevier

NOTICE: this is the author's version of a work that was accepted for publication in *Surface and Coatings Technology*. Changes resulting from the publishing process, such as peer review, editing, corrections, structural formatting, and other quality control mechanisms may not be reflected in this document. Changes may have been made to this work since it was submitted for publication. A definitive version was subsequently published in *Surface and Coatings Technology* (2019) DOI:

<https://dx.doi.org/10.1016/j.surfcoat.2019.125130>

© 2019, Elsevier. Licensed under the Creative Commons Attribution-NonCommercial-NoDerivatives 4.0 International

<http://creativecommons.org/licenses/by-nc-nd/4.0/>

Copyright © and Moral Rights are retained by the author(s) and/ or other copyright owners. A copy can be downloaded for personal non-commercial research or study, without prior permission or charge. This item cannot be reproduced or quoted extensively from without first obtaining permission in writing from the copyright holder(s). The content must not be changed in any way or sold commercially in any format or medium without the formal permission of the copyright holders.

This document is the author's post-print version, incorporating any revisions agreed during the peer-review process. Some differences between the published version and this version may remain and you are advised to consult the published version if you wish to cite from it.

Experimental evaluation of interfacial adhesion strength of cold sprayed Ti-6Al-4V thick coatings using an adhesive-free test method

Dibakor Boruah^{a, b, *}, Ben Robinson^c, Tyler London^c, Huan Wu^c, Heidi de Villiers-Lovelock^d, Philip McNutt^c, Matthew Doré^c, Xiang Zhang^a

^aFaculty of Engineering, Environment and Computing, Coventry University, Coventry CV1 5FB, UK

^bNational Structural Integrity Research Centre (NSIRC), TWI Ltd, Cambridge CB21 6AL, UK

^cTWI Ltd, Cambridge CB21 6AL, UK

^dOerlikon Metco WOKA GmbH, Barchfeld-Immelborn 36456, Germany

*Corresponding Author: Dibakor Boruah

Email address: boruahd@uni.coventry.ac.uk | dibakor.boruah@affiliate.twi.co.uk

Phone number: +44 1223899646, +44 7423674656

Abstract

Cold spray (CS) is a rapidly growing solid-state additive material deposition technique often used for repair of high-value metallic components. This study aims at evaluating the interfacial adhesion strength of cold sprayed Ti-6Al-4V (Ti-64) coatings deposited onto Ti-64 substrates for repair applications. An adhesive-free test method, referred as modified Collar-Pin Pull-off Test was developed based on Sharivker's (1967) original design, in order to overcome the limitations of existing test approaches (both adhesive-based and adhesive-free). This method was designed to allow measurement of adhesion strength of high strength coatings such as CS Ti-64, where adhesion strength is higher than 70-90 MPa. A parametric study was performed to assess the effect of coating thickness, scanning speed, track spacing, toolpath pattern, and substrate surface preparation on the coating adhesion strength. A finite element model was also used to evaluate the stress distribution during the pull-off test, and to check the validity of the proposed test method. The proposed adhesive-free test method was found to be capable of measuring coatings with adhesion strengths beyond the upper limit of conventional adhesive-based methods such as ASTM C633. Among the investigated cases, the highest value of coating adhesion strength was measured around 122 MPa, in the case of CS Ti-64 deposited on ground Ti-64 substrates.

Keywords: Adhesion strength, Cold spray, Coatings, Repairs, Thermal spray, Ti-6Al-4V

1 Introduction

Titanium alloy Ti-6Al-4V (Ti-64) is the most widely used among the various titanium alloys with increasing demand in a wide and diversified range of applications including aerospace, automotive, marine, power generation, sports, and biomedical industries [1]. Ti-64 is desirable in these applications due to its chemical and physical properties *e.g.* higher specific strength and stiffness, excellent fatigue and corrosion resistance, relatively low density, etc. Primarily, Ti-64 alloy is extensively used in many aircraft components such as engine parts, load-bearing airframe structures, landing gear, hydraulic tubing, etc. [2]. Aircraft structural components made of Ti-64 can be prone to in-service damage, such as fretting/galling wear, corrosion pits, fatigue cracks, foreign object damage, etc. [3,4]. To ensure continued airworthiness and high performance, damaged parts need to be replaced or repaired [5]. In general, repair or remanufacturing is a more desired solution than replacement, as it can deliver

significant cost savings between 30 and 70% over the cost of replacement, and also promotes sustainable manufacturing and circular economy [6,7]. With the advancement of solid-state additive deposition technique, Cold Spray (CS) [8], repair/remanufacturing of aerospace components has become more feasible. As a consequence of relatively lower operating temperature in the CS process, the detrimental effects arising from the high-temperature processing (*e.g.* oxidation, compositional changes, phase transformations, and heat affected zones) can be minimized or even eliminated. CS is, therefore, a highly suitable approach for repair of temperature and oxygen sensitive materials, such as titanium, copper, magnesium, and aluminium alloys [7,9]. Although CS has been proven to be effective for dimensional and aesthetic restoration, to repair load-bearing structural components mechanical property specifications are significantly more challenging.

In case of CS Ti-64, a number of research areas have been explored, including metallurgical and mechanical properties [10–13], residual stresses [7], tribological and corrosion properties [1,14,15], and influence of post-deposition thermal treatments [16–18] on the characteristics of the CS deposited material. In addition, the effect of process parameters [4,19–21], powder characteristics [22–25], powder processing [26–28], and substrate surface conditions [29] on various aspects of deposited material have also been investigated. However, there are some areas that have received less attention or could not previously be studied, such as adhesion strength, due to the lack of a suitable test method. Therefore, the effect of process parameters, substrate surface preparation, and coating thickness on the adhesion strength is currently unknown.

Coating-substrate adhesion strength is a key commonly measured property as a part of structural integrity assessment of load-bearing repair components. However, due to higher interfacial adhesion strength between CS deposited Ti-64 particles and the Ti-64 substrate, conventional adhesive based test methods (*e.g.* ASTM C633 [30] and ISO 14916 [31]) are not suitable to measure the adhesion strength. Many researchers [4,11,32] have attempted to measure the adhesion strength in the case of CS Ti-64 deposited on Ti-64 substrates using the ASTM C633 standard [30]. It was reported that specimens failed at the adhesive bond-line instead of the coating-substrate interface, which demonstrates that the adhesion strength is higher than the tensile strength (adhesive strength) of the adhesive used to bond the samples [4,11]. In addition to CS Ti-64, recent advances in the thermal spray technology have resulted in coating-substrate adhesion strengths exceeding the maximum limit (70-90 MPa) of the typically used adhesives and the measured values are often quoted as ‘greater than’ the adhesive strength of the adhesive used. For example, CS coated Cu on 316L, Cu, and Al alloy substrates [33,34], CS coated Al-Al₂O₃ on Al7075 [35], CS coated CP-Ti on mild steel substrate [36], and HVOF sprayed IN718 on IN718 [37].

There is a range of existing test methods for the determination of adhesion strength in thermal spray coatings, which can be categorised into mainly two types- (1) adhesive-based test methods [4,11,30,31,38–41], and (2) adhesive-free test methods [11,33,34,41–49] (see Appendix A1). Among these currently used testing approaches, Tensile Adhesion Test (TAT) [30,31], is the most commonly used owing to its efficiency and simplicity. However, as it uses an adhesive, it cannot be used when coating-substrate adhesion strength exceeds the strength of the adhesive (*i.e.* 70-90 MPa). Moreover, adhesive-based methods are susceptible to other issues, such as improper curing, degradation,

penetration of the adhesive to the coating, mixed-mode failure, misalignment problem, etc., which makes determination of adhesion strength challenging. The existing adhesive-free methods also have limitations. Scratch Test [44] is especially for the assessment of very thin coatings ($\leq 30 \mu\text{m}$). Interfacial Indentation Test [45] requires very complex set-up and also requires a minimum coating surface roughness of $4\text{-}8 \mu\text{m R}_a$, which limits the applicability of the test. The main issue with the Peel Test [46,47] is the limited availability of appropriate foils. Availability of the limited range of foils restricts its scope for testing coating/substrate combinations. There is also question of whether the coating deposited on the test foil is representative of a coating on the relevant component, due to factors such as thermal conductivity. A significant issue with the Tie Bar testing approach is mixed-mode failure due to the nature of its test piece arrangement [38]. Laser Shock Adhesion Test (LASAT) [49] is a promising method for measurement of adhesion strength, however, limited by its requirement for expensive pulsed laser and velocity laser interferometer equipment. Moreover, it is challenging to develop an appropriate underpinning theoretical model [49]. Recently, adhesive-free methods such as modified ASTM E8 [11,48], and modified ASTM C633 [33,34] were found to be used to measure the true adhesion strength. Tan et al. [11] have measured adhesion strength using a modified ASTM E8 method for Ti-64 coatings deposited Ti-64 substrates, which was found to be 90 MPa. However, these adhesive free-methods [11,33,34,48] require a very thick coating ($\sim 5 \text{ mm}$ [11,33]) and post-deposition machining to get desired dimensions; which is time consuming and expensive. The thicker coatings induce higher residual stresses causing poorer adhesion to the substrate, which may result in interface crack or delamination [4,50], as also explained in [7,51] using a parametric study on residual stresses by means of both experimental and analytical predictions. In addition, post-deposition machining of the test specimens may itself introduce defects into the coating and/or the coating-substrate interface, especially for the materials that are more challenging to machine such as titanium alloys. Moreover, due to the significant thickness of the coating required to carry out the test, results may not be representative of the coating in application which could be significantly thinner. Therefore, currently, none of the commonly used adhesive-free methods are appropriate for measuring adhesion strength that exceed 70-90 MPa. Moreover, existing adhesive-free methods are not suitable to investigate the influence of the coating thickness, substrate surface conditions, and process parameters on the adhesion strength of thermal spray or CS coatings with higher adhesion strength. Hence, an alternative test is required to measure the true adhesion strength of high-strength coatings, particularly for load bearing repairs such as CS Ti-64 coatings deposited on Ti-64 substrates.

In this study, a suitable adhesive-free test method was chosen for further improvement, which was first proposed in 1967 by Sharivker [42]. This test method with certain modifications appeared as promising for the assessment of interfacial adhesion strength of thick CS coatings. Therefore, a modified design of the adhesive-free test method was developed based on Sharivker [42], Lyashenko et al. [43], and ASTM C633 [30]; which has been prototyped, performed testing trials and optimised iteratively in different stages. The effective coating-substrate adhesion strength was evaluated for CS Ti-64 coating deposited on Ti-64 substrates in terms of the effect of the (i) coating thickness (0.4 mm to 6 mm), (ii) process parameters (toolpath pattern, scanning speed, and track spacing), and (iii) substrate surface preparation

(grit blasted, as-machined, and ground). Furthermore, a finite element analysis was performed to model the test and evaluate stress distribution along the interface during the pull-off loading.

2 Methodology

2.1 Feedstock powder and substrate material

A commercially available gas atomised Ti-64 powder, LPW -32+16 μm ($d_{10} = 16.89 \mu\text{m}$, $d_{50} = 23.12 \mu\text{m}$, $d_{90} = 31.69 \mu\text{m}$) provided by LPW Technology Ltd. (Cheshire, UK), was used. The particle size distribution, powder morphology, and microstructure of the powder used are presented in Figure 1a-c [7]. Substrate material was Mill Annealed Ti-64 round bar, supplied by Dynamic Metals Ltd. (Bedfordshire, UK). Figure 1d-f shows substrates with three different treatments (grit blasted, as-machined, and ground) along with their respective surface roughness values. The surface of the prepared test specimens was measured using a 3D surface profilometer (Alicona InfiniteFocusSL) as per ISO 4288:1996 [52]. The analysis was performed using the associated IF Measure Suite software. Chemical compositions of the powder and substrate material are presented in Table I.

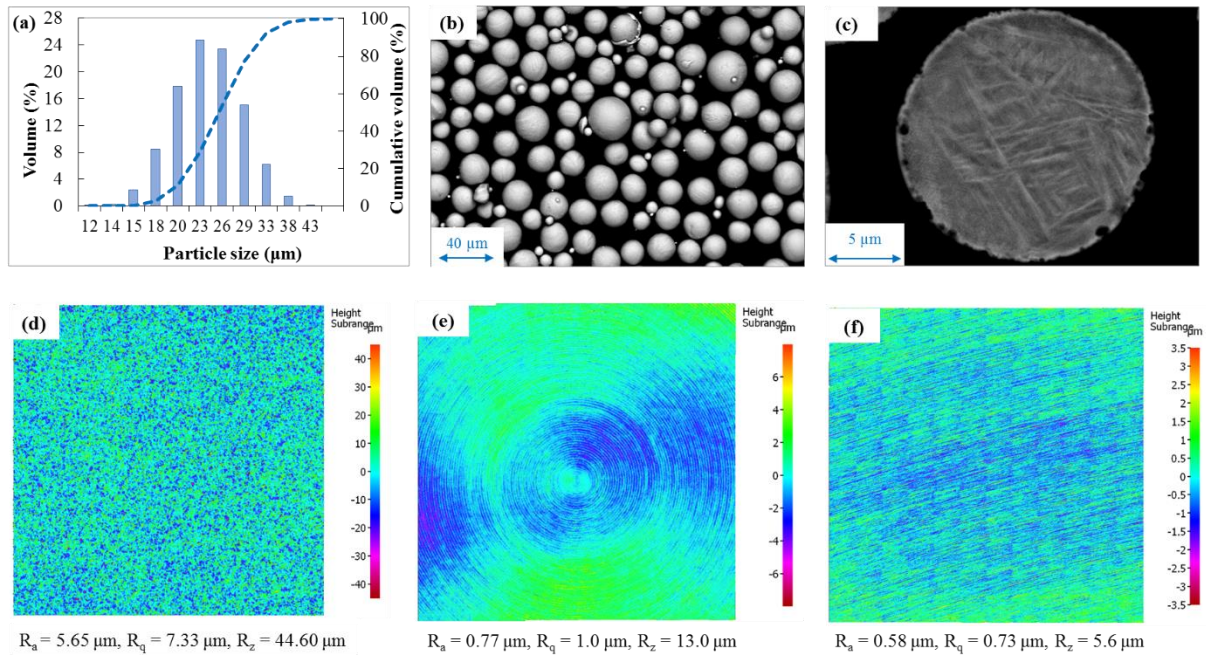


Figure 1: Characteristics of the gas atomised LPW -32+16 Ti-64 powder: (a) particle size distribution, (b) powder morphology, (c) microstructure showing the rapidly solidified α' martensitic needles [7]; 3D profilometry measured by Alicona for different substrate surface preparation: (d) grit blasted, (e) as-machined (faced on Lathe machine), (f) ground with 320 grit paper.

Table I: Chemical compositions (mass %) of Ti-64 powders and mill annealed substrate material

Powder/ substrate	Ti	Al	V	Fe	O	Si	Sn	Cr	Ni	Others
LPW -32+16 powder	Balance	6.48	4.03	0.17	0.17	0.01	0.02	<0.01	<0.02	<0.01
Mill annealed substrate	Balance	6.32	4.16	0.20	0.13	0.02	<0.01	0.02	0.01	<0.01

2.2 Specimen preparation and characterisation

All specimens were manufactured using Impact Innovation 5/11 high-pressure CS system at TWI Ltd, Cambridge, UK (Figure 2a). Key process parameters used for CS deposition are shown in Table II.

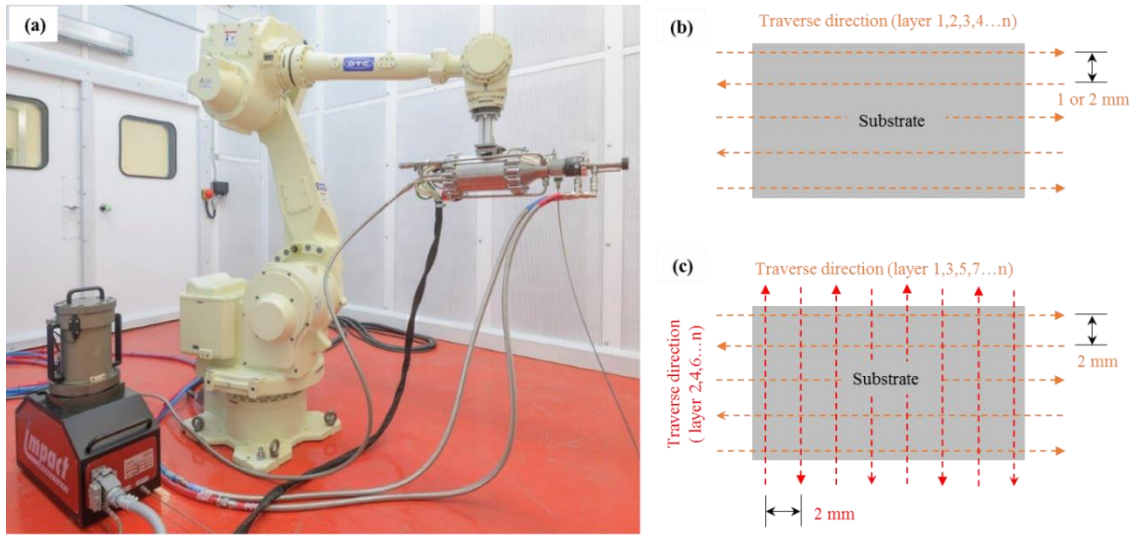


Figure 2: (a) Impact Innovation 5/11 high pressure CS system at TWI Ltd; CS toolpath patterns: (b) horizontal raster, and (c) cross-hatch [7].

Table II: Spraying conditions used to deposit Ti-64 CS coatings

CS system setup	Gun	CS system	Impact 5/11
		Nozzle	T24-SiC
		Pre-chamber	Long (128.6 mm)
		Gas pressure (MPa)	5
		Gas temperature (°C)	1100
	Powder feeder	Dosing disk rotation speed (rpm)	3
		Powder feed rate (g/min)	24.67
		Carrier gas flow rate (m ³ /hr)	3
	Nozzle cooling medium	Water	
Robot and toolpath setup	Gun traverse or scanning speed (mm/sec)	500 or 300 (see Table III)	
	Track spacing (mm)	1 or 2 (see Table III)	
	Spray angle	90°	
	Standoff distance (mm)	30	
	Toolpath pattern	Horizontal raster or cross-hatch (Figure 2b-c, also see Table III)	
Surface preparation	Grit blasted ¹ , As-machined ² , and Ground ³ (Figure 1d-f, also, see Table III)		

¹ Degreased, and grit blasted using mechanised WC with nominal size 44 μm at an angle of 60°. Surface roughness of the grit blasted surface was measured as $R_a = 5.65 \mu\text{m}$, $R_q = 7.33 \mu\text{m}$, $R_z = 44.60 \mu\text{m}$.

² As-machined ($R_a = 0.77 \mu\text{m}$, $R_q = 1.0 \mu\text{m}$, $R_z = 13.0 \mu\text{m}$).

³ Ground with 320 alumina grit paper ($R_a = 0.58 \mu\text{m}$, $R_q = 0.73 \mu\text{m}$, $R_z = 5.6 \mu\text{m}$).

2.3 Coating-substrate adhesion strength

2.3.1 Modified Collar-Pin Pull-off Test

The adhesive-free test method developed in this study roots back from the 1960s. The original idea of the proposed adhesive-free test method was taken from Sharivker [42] (Figure 3a) and Lyashenko et al. [43] (Figure 3b), which was later mentioned as “Plug” method by Lyashenko et al. [53]. In this method, a “Pin” is placed into the “Collar” such that the two surfaces are flush and the two are then coated. A load is then applied to the Pin until it is removed, resulting in the coating to dis-bond from the Pin head area. The adhesion strength can then be calculated from the load required to remove the Pin. As can be seen from Figure 3, Sharivker’s [42] specimen consist of a Cylindrical Pin section (or plug [53], or base [42]) and a Collar (or washer [42], or disc [43], or plate [53]); on the other hand, Lyashenko’s [43] design consisting of a Conical Pin acting as a substrate, which is supported by a system comprising of a Concentric Disk, alignment pin and ball bearings. These two methods were first proposed and trialed during 1967-1972, but ultimately did not reach wide use, probably due to the complex design and/or its then application to the testing of less challenging coatings. However, with the improvements in machining standards, this test appeared to be a promising method for measuring adhesion strength of thick CS coatings.

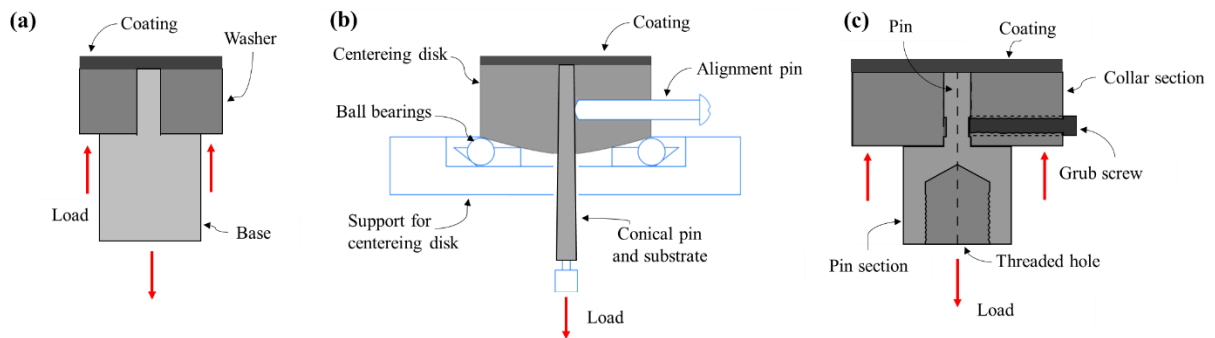


Figure 3: Adhesive-free adhesion test specimens proposed by: (a) Sharivker [42], (b) Lyashenko et al. [43]; (c) a hybrid design (Prototype 1) developed by TWI Ltd [54], which is a mixture of Sharivker [42], Lyashenko et al. [43], and ASTM C633 [30].

In this study, a modified test method has been developed, which is a hybrid version of the two methods proposed by Sharivker [42] and Lyashenko et al. [43]. The initial design (Prototype 1) is shown in Figure 3c, which comprises of a Pin section and Collar section with a grub screw. Trial tests were performed to understand the feasibility of this test method [54]. Subsequently, the initial design (Prototype 1) was further improved and optimised iteratively for easy integration with conventional tensile testers and ASTM C633 [30] test fixtures. Drawing and experimental set-up of the final design (Prototype 2) are presented in Figure 4a,b. The specimen consists of mainly two parts: the Pin section, and the Collar section with an M16 threaded base such that conventional ASTM C633 tensile testing equipment and procedures can be used for testing minimising misalignment/shear effects. The Pin diameter was set at 5 mm, and the height of the Pin section was set at 14 mm with overall height of the Pin section 38.1 mm (which is same as ASTM C633). Before assembling the Pin and Collar, they were ultrasonically cleaned to remove remnant cutting fluid and any remaining oil/grease from the machined parts, which have been found to be a source of contamination if not fully removed. The components were dried and assembled,

ensuring that the base of the Collar section meets the base of the Pin, and secured with two grub screws at 180° to each other (instead of the one grub screw used in Prototype 1) to prevent relative movement during handling and coating deposition process. The top face of the specimens was dry ground until the surface is completely flush. After depositing the coating, the following sequence was used to test a coated assembly- the sample was placed into the mechanical test apparatus, then grub screws were removed, and finally pulled at a displacement rate of 1 mm/min until failure. The failure load is anticipated to be significantly lower in the proposed test method due to the small Pin diameter.

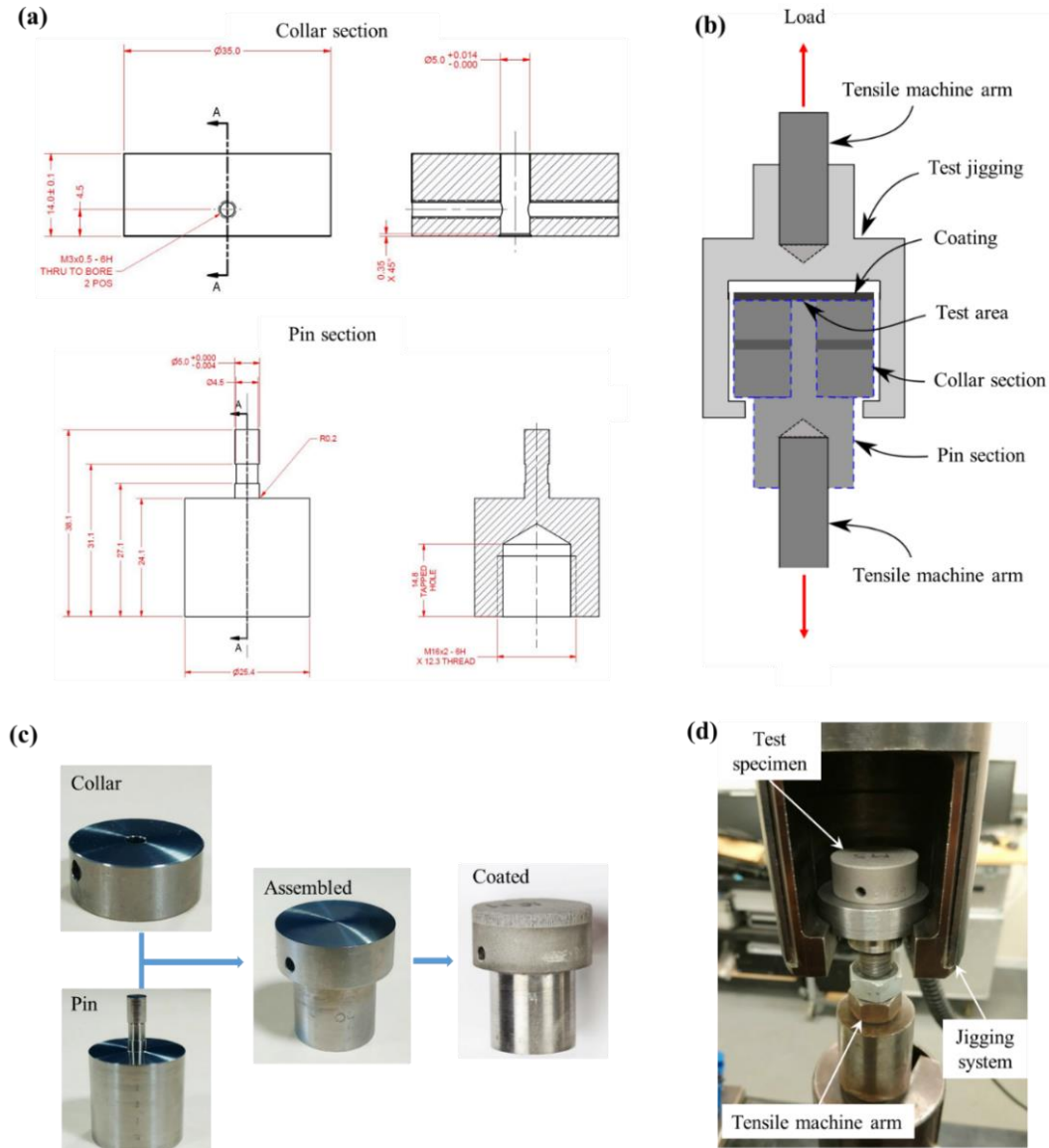


Figure 4: The proposed adhesive-free adhesion test method termed as modified Collar-Pin Pull-off Test (Prototype 2): (a) CAD drawing of the test specimen parts, Collar section and Pin section (dimensions in mm), (b) schematic of the experimental set-up, (c) specimen preparation process: cleaned machined parts (Collar and Pin) assembled and secured with two grub screws followed dry grinding the top surface until finish, and a CS deposited specimen (Ti-64/Ti-64), and (d) custom test fixture for uniaxial loading.

2.3.2 Parametric study on the coating-substrate adhesion strength

A parametric study was performed to determine the effect of coating thickness, scanning speed, track spacing, toolpath pattern, and different substrate surface preparation on the coating adhesion strength for Ti-64 coatings deposited on Ti-64 substrates. As presented in Table III, a range of tests was

performed for 13 different conditions (CS-1 to CS-13) with three specimens produced for each condition. Moreover, due to the configuration of the proposed test method, there might be some inherent friction between the Pin and Collar interfaces during loading, particularly, titanium alloys often suffer from galling. This friction could contribute to the increase of the force required to de-bond the coating. Therefore, one more set of tests (UC-14) were conducted for assembled but uncoated specimens.

2.3.3 Coating-substrate cross-section analysis

A Collar-Pin Pull-off Test specimen (deposited using same spraying and substrate preparation conditions as CS-13, as presented in Table III) was cross-sectioned in the as-deposited condition using a precision diamond saw, and mounted in Epofix cold-curing acrylic resin, and ground/polished to 0.25 μm for optical microscopy, to determine if any coating defects are observable at the Collar-Pin interface. Moreover, etched optical micrographs were taken for the cross-sections of the interfaces with three different substrate surface preparations *i.e.* grit blasted, as-machined (faced on Lathe machine), and ground with 320 grit paper.

2.3.4 Finite element modelling

To support the experimental activities, finite element analysis (FEA) was undertaken to quantify the stress state in the test setup for Prototype 2. Taking into account the axisymmetry nature of the test setup, a two-dimensional, axisymmetric model was created in Abaqus/CAE. The finite element model is shown in Figure 5a. The model was meshed entirely with quadratic displacement, axisymmetric, reduced-integration elements (type CAX8R in Abaqus) with a characteristic mesh size of 0.10 mm. The cases analysed included a 5 mm diameter Pin with three different coating thicknesses 0.9, 4.3, and 6.0 mm, respectively, to study the effect of coating thickness on stress distribution along the interface. Similarly, a 15 mm diameter Pin with coating thickness 4.3 mm was also modelled to see the effect of Pin diameter on stress distribution.

To approximate the test conditions, the coating (red region) was fully bonded to the Collar (blue region) and the Pin (light blue region) as shown in Figure 5a. Sliding contact was allowed between the Pin and Collar, and the mesh was refined in the region of the local notch stress at the Collar-Pin-Coating triple junction (see Figure 5b). The load and boundary conditions for the finite element model are- (i) all edges along the axis of symmetry were restrained in the radial direction, (ii) the bottom of the Collar was restrained in the vertical direction to represent a support, and (iii) the bottom of the Pin was kinematically coupled to a reference point which was then displaced in the axial direction (whilst all other degrees of freedom were restrained). Each simulation was analysed under static conditions, and the nominal applied stress was calculated by using Eq. 1. As shown in Figure 5c, the red line represents the axisymmetric boundary condition (radial restraints with displacements in the x-direction restrained); the light blue line represents a vertical support of the Collar with displacements in the y-direction restrained); and the green lines represent the kinematic coupling between the bottom face of the Pin to a reference point which was displaced in the negative y-direction (axially displaced).

$$\text{Nominal applied stress} = \frac{\text{Reaction force arising due to displacement applied at the bottom of the Pin}}{\text{Nominal cross-sectional area of the Pin}} \dots\dots\dots (1)$$

Table III: Specimen details for measuring coating-substrate adhesion strength using Collar-Pin Pull-off Test

Specimen type	No. of layers	Coating thickness (mm)	Toolpath pattern	Scanning speed (mm/s)	Track spacing (mm)	Average layer thickness (μm)	Substrate preparation	Delamination	No. of specimens
CS-1	4	0.4	Horizontal raster	500	2	~107	Grit blasted	No	3
CS-2	8	0.9	Horizontal raster	500	2	~107	Grit blasted	No	
CS-3	16	1.7	Horizontal raster	500	2	~107	Grit blasted	No	
CS-4	24	2.6	Horizontal raster	500	2	~107	Grit blasted	No	
CS-5	32	3.4	Horizontal raster	500	2	~107	Grit blasted	No	
CS-6	40	4.3	Horizontal raster	500	2	~107	Grit blasted	No	
CS-7	48	5.1	Horizontal raster	500	2	~107	Grit blasted	Partial delamination	
CS-8	56	6.0	Horizontal raster	500	2	~107	Grit blasted	Partial delamination	
CS-9	16	1.7	Cross-hatch	500	2	~107	Grit blasted	No	
CS-10	16	2.7	Horizontal raster	300	2	~167	Grit blasted	Partial delamination	
CS-11	16	3.4	Horizontal raster	500	1	~213	Grit blasted	No	
CS-12	24	2.6	Horizontal raster	500	2	~107	As-machined	No	
CS-13	24	2.6	Horizontal raster	500	2	~107	Ground with 320 grit paper	No	
UC-14	Uncoated								

Young's modulus (E) value of the mill annealed Ti-64 was used for the Pin and Collar section (113.32 GPa). For the coating material, E value was used 88.48 GPa [7], measured using the Impulse Excitation technique as per ASTM E 1876 [55]. Poisson's ratio (ν) was assumed as 0.34 for both the materials

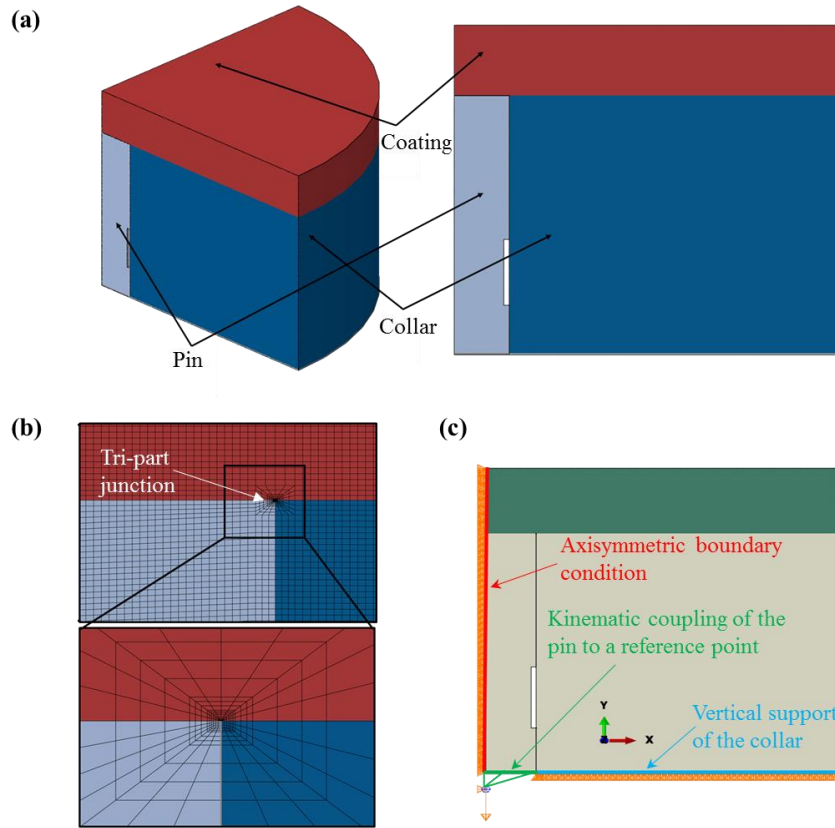


Figure 5: (a) Finite element model showing the three-dimensional shape (left- quarter symmetry, right-axisymmetric plane). (b) FE mesh with a characteristic element size of $0.1 \times 0.1 \text{ mm}^2$ showing the refinement in the region local to the notch at the Collar-Pin-Coating tripple junction. (c) Illustration of the loads and boundary conditions

3 Results and iscussion

3.1 Interfacial adhesion strength

Figure 6a-e shows the results of the parametric study on the influence of geometrical and process variables on the coating-substrate adhesion strength. The effect of coating thickness (0.4 to 6.0 mm, CS-1 to CS-8, Table III) on the adhesion strength is shown in Figure 6a. A correlation of adhesion strength increasing from $32.2 \pm 3.4 \text{ MPa}$ to $107.2 \pm 7.6 \text{ MPa}$ with coating thickness, 0.4 to 4.3 mm, was observed. Adhesion strength was then observed to decrease to $74.8 \pm 25.1 \text{ MPa}$ with further coating thickness increase up to 6.0 mm. At the lowest thickness (0.4 mm) the coating showed mixed-mode failure, *i.e.* coating failed cohesively at the centre, and along the interface near the edges of the Pin. Mixed-mode failure resulted in a hole (smaller than that of the Pin diameter) in the coating surface (Figure 7a), which was due to very high non-uniform stress distribution along the interface, especially negative or very lower stress level acting at the centre region of the Pin (see FEA results for thin coatings in Section 3.3, Figure 9). For all other coating thicknesses (0.9 to 6.0 mm) specimens failed at the coating-substrate interface (Figure 7b). Thinner coatings with 0.9 and 1.7 mm thickness showed lower adhesion strength

although they failed at the coating-substrate interface. Which can also be explained from the FEA results as presented section 3.3, *i.e.* higher non-uniformity in stress distribution at the Pin-Coating interface plus very high stress concentration at the Collar-Pin-Coating junction, creating a notch during the separation of the Pin and Collar during pull-off leading to premature failure. Nominal adhesion strength (friction converted into strength) for the uncoated specimens (UC-14) was measured to be 3.3 ± 0.9 MPa, which is within or close to the scatter range of the adhesion strength values measured for Ti-64 coatings, irrespective of the spraying conditions. Deduction of the nominal adhesion strength value of the uncoated specimens (*i.e.* 3.3 MPa) from the adhesion strength results may be an option while analysing the test data. Generally, such small frictional stress between the Pin and Collar is not expected to have a considerable effect on the validity of the test results, especially when expected adhesion strength is very high. However, there might be external forces acting on the Pin during the coating deposition process, *e.g.* inclusions at the sidewall between the Pin and the Collar (see section 3.2, Figure 8c). Therefore, the effect of sidewall friction on the overall adhesion strength is unclear, and need further investigation. Another alternative for avoiding the sidewall friction is improving the design of the testing set up by replacing the Cylindrical Pin with a Conical Pin, as recommended by [43].

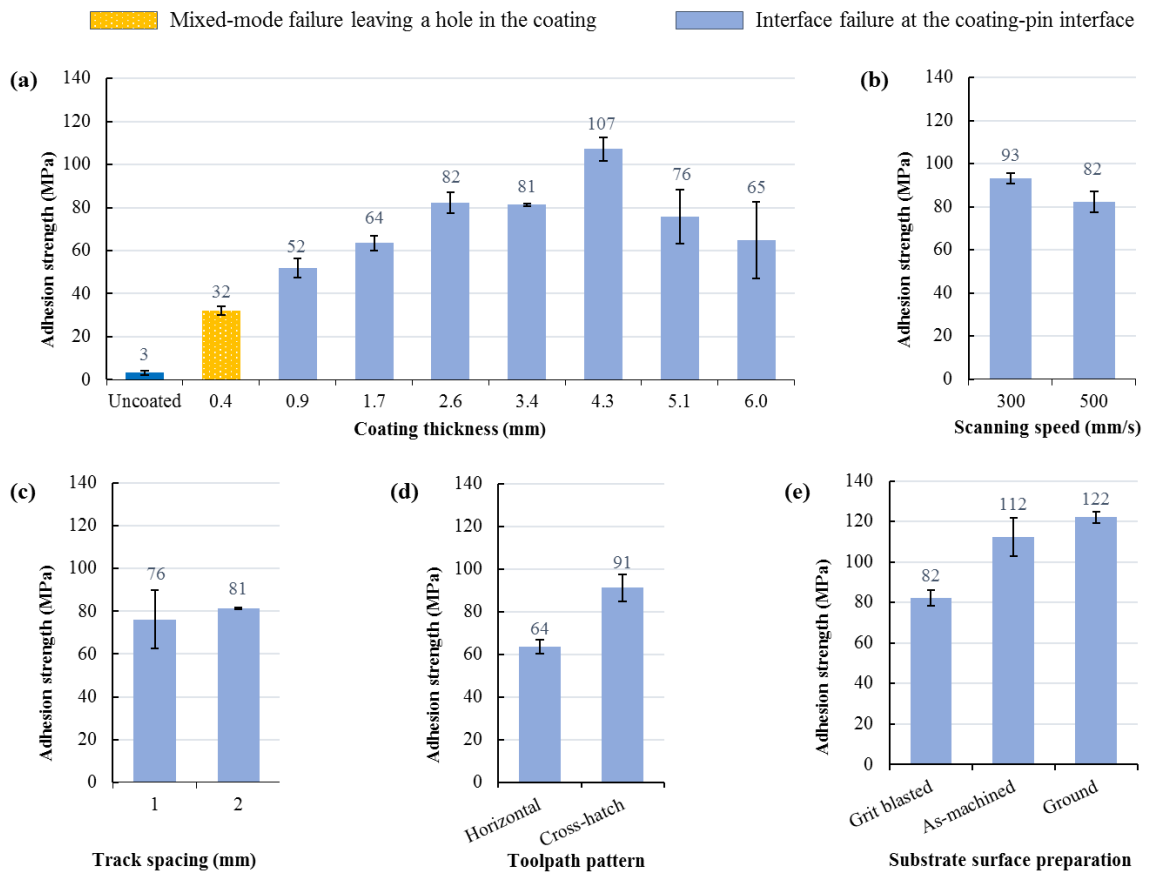


Figure 6: Coating-substrate adhesion strength: effect of (a) coating thickness (UC-14, CS-1 to CS-8), (b) scanning speed (CS-10, CS-4), (c) track spacing (CS-11, CS-5), (d) toolpath pattern (CS-3, CS-9), and (e) substrate surface preparation (CS-4, CS-12, and CS-13); see Table III for specimen details. Error bars in (a-e) represents the standard error of the mean.

Figure 6b shows the effect of scanning speed on the adhesion strength. Both sets of specimens had a coating thickness of ca. 2.6 mm and were produced at scanning speeds of 300 mm/s (CS-10) and 500 mm/s (CS-4). Adhesion strength was found to be around 13% higher at the lower scanning speed. However, partial delamination (fine cracks at the edges, see Figure 7c) were found at the interface for the specimens deposited at 300 mm/s. This is thought to be due to the higher deposition rate (increased average layer thickness of $\sim 167 \mu\text{m}$ for coatings deposited at 300 mm/s, compared to $\sim 107 \mu\text{m}$ 500 mm/s) that resulted in higher residual stresses at the interface as explained in [7,51]. In contrast, no delamination was found at the interface in the specimen deposited at 500 mm/s ($\sim 107 \mu\text{m}$ average layer thickness). Therefore, theoretically, the adhesion strength values should be lower for specimens deposited at 300 mm/s. Significant reduction in adhesion strength at lower traverse scanning speed was also reported by Tan et al. [4]. From the temperature analysis reported in [4], the substrate temperature decreases with the increase in gun traverse speed, in other words, the largest heat accumulation at the lowest scanning speed. The maximum substrate temperature at traverse speed 100, 300 and 500 mm/s for coating deposition were reported to be 366, 354, and 315 °C, respectively. As stated in [4], rapid thermal build-up as a consequence of slow traverse speed allows sufficient time for chemical reaction, which may result in the formation of an oxide layer. Presence of thick oxide film at the substrate may have a negative effect on spraying particle bonding to the substrate. Moreover, higher non-uniformity in thermal distribution was observed at lower traverse speed, which may result in higher residual stresses caused by non-uniform thermal expansion and shrinkage originating from thermal fluctuations at lower scanning speed [4], along with the effect of average layer thickness [4,7,51]. However, in this study, contradictory results were observed (*i.e.* higher adhesion strength at lower scanning speed), which may be explained with the fact that higher residual stress leads to delamination at the edges of the interface, leaving the centre of specimen being unaffected and relatively stress free where the Pin is attached to the coating.

Figure 6c shows a comparison between two different track spacing (1 mm and 2 mm) on specimens with the same coating thickness ca. 3.4 mm (CS-11 and CS-5). As expected, average adhesion strength was lower with larger scatter for the specimens deposited with 1 mm track spacing with higher coating thickness ($\sim 213 \mu\text{m}$ average layer thickness), as compared to the 2 mm track spacing ($\sim 107 \mu\text{m}$ average layer thickness). In the case of 1 mm track spacing, a larger portion of each deposited track gets overlapped, *i.e.* the core of the spraying jet having higher particle velocity (in the exit plume of the nozzle) [56] is overlapped with the edges of previously deposited tracks instead of the substrate, which may have negative effect on the direct adhesion of the spraying particle to the substrate. Then again, tamping or hammering effect at the edges of a previously deposited track by the core of a new track (higher particle velocity zone) may also lead to higher adhesion of the loosely bonded edges of the previous track with the substrate. On the other hand, in the case of 2 mm track spacing, the core of the spraying jet is directly hitting the substrate with less area being overlapped with the edges of previously deposited tracks causing adhesion of the spraying particles directly to the substrate with higher impact. Therefore, the effect of track spacing on the interfacial adhesion strength is ambiguous. Moreover, from

the statistical point of view, there is no difference between the two populations, since the error bars overlaps and the overlapping region includes the means of the sample size. However, the higher scatter in case of 1 mm track spacing may be due to higher thickness per layer leading to higher residual stresses at the interface region resulting in lower adhesion strength in some cases. Effect of layer thickness on residual stresses can be explained using an analytical model discussed in our previous work for various residual stress build-up mechanisms namely peening dominant [51], thermal mismatch dominant [51], and quenching dominant CS processes [7]. Therefore, from the point of view of average thickness per layer, 2 mm track spacing with lower thickness per layer is better for maintaining lower residual stresses at the interface and can contribute towards higher coating adhesion strength.

Figure 6d compares specimens deposited using two different toolpath patterns, horizontal raster (CS-3) and cross-hatch (CS-9). The coating-substrate adhesion strength was found to be 42% higher using the cross-hatch toolpath, which may be due to the lower level of residual stresses near the interface region as shown in previous work [7]. This can be explained based on a hypothesis that the cross-hatch spraying pattern evens out the bending moment (and consequently the residual stress) originating from each layer deposited *via* alternating spraying direction normal to each other resulting in a net decrease in the residual stresses, which improve coating adhesion. See Appendix A2 (Figure A2a,b) or our previous work [7] for more information on the effect of process and geometrical variables on residual stresses induced by CS Ti-64 deposited on Ti-64 substrates.

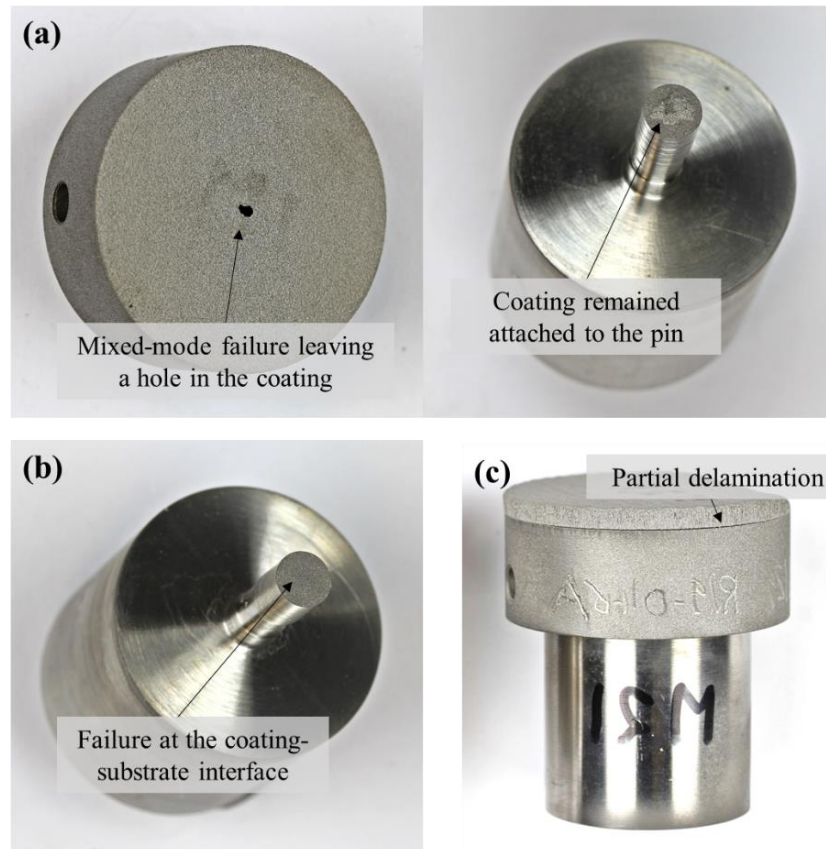


Figure 7: Tested adhesion specimens showing (a) mixed-mode failure leaving a hole in the coating (0.4 mm thick, CS-1) while coating remained attached to the centre region of the Pin, (b) interface failure at the Pin-Coating interface leaving an uncoated pin area (CS-5 as an example for all cases from CS-2 to CS-13), (c) partial delamination in the interface deposited at 300 mm/s scanning speed (CS-10).

Figure 6e shows the effect of substrate surface preparation (*i.e.* grit-blasted, as-machined, or ground) on the coating adhesion strength. Adhesion strength values were 35-50% higher in the as-machined and ground specimens as compared to the grit-blasted specimens. Grit-blasting is generally performed prior to spraying, as it is believed that a rougher substrate increases the surface area for bonding and contributes to the mechanical interlocking of the sprayed particles with the substrate. However, lower adhesion strength in the case of CS Ti-64 deposited on grit-blasted substrate may be caused by the work hardening phenomenon associated with the grit blasting process, whereby the impact of the WC grit particles on the surface cause work hardening of the substrate. This work hardening can effect deformation and bonding of the spraying particles with the substrate [57]. Embedded grit in the substrate may also form a barrier to metallurgical bonding between the deposited particles and the substrate.

3.2 Coating-substrate cross-section analysis

Figure 8a-c shows a cross-sectioned test specimen, with no apparent defects in the Collar-Pin interface region. There is a fine crack observed at the Collar-Pin-Coating junction as shown in Figure 8c, which may occur while handing the specimen for cross-sectioning, mounting and/or polishing, or due to relaxation of residual stresses. However, it was unclear what effect (if any) this may have on the loading of the test specimen. Additionally, cross-sectional images (etched microstructure) of the interfaces with three different substrate surface preparations (grit blasted, as-machined, and ground) are presented in Figure 8d-f.

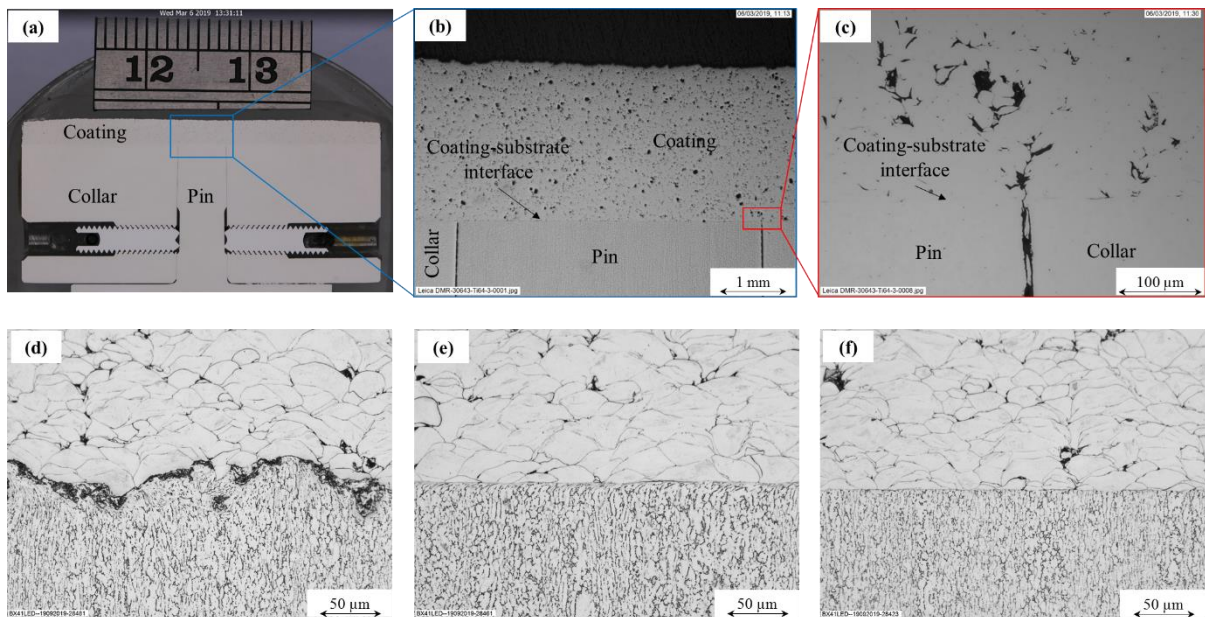


Figure 8: (a) Macro photograph of a cross-sectioned Ti-64 coated Collar-Pin Pull-off Test specimen in the assembled condition; optical micrograph (b) showing the coating structure at the Collar-Pin interfaces, and (c) Collar-Pin-Coating junction; cross-sectional optical micrograph showing coating-substrate interface for different substrate surface preparation: d) grit blasted, (e) as-machined (faced on Lathe machine), (f) ground with 320 grit paper.

3.3 Finite element analysis: effect of coating thickness and Pin diameter

Stress distribution in the coating-substrate interface under nominal applied stress of 52 MPa was modelled for a Pin with 5 mm diameter at three different coatings thickness. To understand the effect of coating thickness on the stress distribution, three different coating thicknesses were chosen- (i) 0.9 mm,

the thinnest coating thickness with interface failure, (ii) 4.3 mm, the coating thickness with maximum measured adhesion strength value, and (iii) 6.0 mm, the maximum coating thickness investigated in this study. To model the effect of Pin diameter on stress distribution, the Pin diameter was increased from 5 mm to 15 mm while keeping all other dimensions same for coating thickness 4.3 mm.

Figure 9a-c shows the stress distribution for the specimen with 5 mm Pin diameter with coating thicknesses 0.9, 4.3, and 6.0 mm, respectively. Under nominal applied stress of 52 MPa, the axial (normal) stresses acting along the Pin-Coating interface was found to be non-uniform with significantly higher stresses at the edges of the Pin and decreased towards the Pin centre. It was found that across a large portion of the Pin-Coating interface experienced significantly lower stresses reaching -3.5, 33.9, and 36.8 MPa at the centre area of the Pin for coatings with thicknesses 0.9, 4.3 and 6.0 mm, respectively. The negative stress values at the centre of the Pin may be the reason behind mixed-mode failure in the case of 0.4 mm thick coating as shown in Figure 7a. Moreover, for all three cases, the localised stress near the Collar-Pin-Coating junction was much higher. Very high stress concentration at the tri-part junction and lower-than-nominal stress across the remainder of the interface (specially, at the centre region of the Pin) could create a local notch at the interface close to the tri-part junction due to the Pin being separated from the Collar during pull-off loading, where yielding and failure will initiate leading to premature failure.

A similar trend in stress distribution was also observed in the case of 15 mm diameter Pin with coatings thickness 4.3 mm, as shown in Figure 9d. However, the area of the Pin (15 mm) that experienced lower stresses was much larger than that for the Pin with a smaller diameter (5 mm). Increasing the Pin diameter to 15 mm resulted in an interfacial stress state that was significantly less uniform than that for the 5 mm Pin diameter. This is due to the stress concentration at the tri-part junction of the 15 mm Pin with larger Pin area, providing a larger region in the interface with reduced stresses reaching 5.3 MPa at the centre, while for a 5 mm Pin it was 33.9 MPa at the centre, under a nominal applied stress of 52 MPa. The significant reduction in adhesion strength values with the increasing in Pin diameter was also reported in [53].

Figure 9e shows a comparison (among a-d) of the stress distribution along the interface from the Collar-Pin-Coating junction to the centre of the Pin. The “steps” in this curve were due to the fact that the coating and Pin have different Young’s moduli. As a consequence, the stress being extrapolated along the interface of nodes with values of stress from elements on one side having material properties of the coating and elements on the other side having the pin material properties, resulting in two stress values at each nodal position. From Figure 9e, it is obvious that the lesser the coating thickness the higher the non-uniformity in stress distribution; similarly, the higher the Pin diameter the higher the non-uniformity in stress distribution along the Pin-Coating interface. Higher non-uniformity in stress distribution along the Pin-Coating interface (having lower-than-nominal stress at the centre region) and very high stress concentration at the tri-part junction may lead to premature failure resulting in a lower adhesion strength (lower than the true value). This effect would be more significant for thinner coatings with lower stiffness or considerably larger Pin diameter comparing to the coating thickness. Moreover, higher non-

uniform stress distribution may also cause cohesive or mixed-mode failure specifically for thinner coating. Therefore, for a thin coating, the result obtained from the adhesion test would represent a lower value than the 'true' coating adhesion strength. These results would suggest that a Pin diameter of <5 mm could be used to achieve a more uniform stress state across the interface, especially for thinner coatings <1.7 mm. However, using a smaller Pin diameter would decrease the cross-sectional area being tested and therefore make results significantly more sensitive to any local defects or imperfections in the coating and Pin interface. The Prototype 2 design is therefore a compromise between these two factors.

3.4 Validity of the modified Collar-Pin Pull-off Test

While mechanical testing has shown that the proposed test method is capable of measuring coatings with adhesion strength >90 MPa with comparable data point scatter to that of conventional TAT arrangements, computation modelling has demonstrated non-uniform stress distribution at the test area of the coating-substrate interface. This means that the values measured are not representative of the true adhesion strength of the coating, particularly for thinner coatings such as 0.4 mm and 0.9 mm thick coatings. As reported by Sharivker [42], practically, adhesion strength decreases linearly with the increase in coating thickness for thermal sprayed coatings, however, the slope of linearity may vary for different coating and substrate material. Similar results were also reported for thermal spray [50] and CS coatings [58]. However, with the proposed test method, adhesion strength increases with the coating thickness up to a certain thickness (4.3 mm for CS Ti-64 coatings shown in Figure 10). This contradictory trend of adhesion strength with up to 4.3 mm thick coating can be explained by the FEA results showing very high non-uniformity in stress distribution along the interface, as discussed in section 3.3. In Figure 10, further increase in coating thickness beyond 4.3 mm, adhesion strength started to fall rapidly following a close to linear trendline. The reduction in measured adhesion strength value above 4.3 mm coating thickness is due to higher residual stresses, but not because of non-uniformity in stress distribution at the Pin-Coating interface. Similar trend of adhesion strength against coating thickness was also reported in [42,43,53], for a range of thermal sprayed coating-substrate assemblies, measured using similar test methods as this study.

The adhesion strength vs. coating thickness plot shown in Figure 10, can be categorised into two zones. Zone "A" represents the coating thickness range (*i.e.* coatings with thicknesses lower than 4.3 mm in this study), where values measured represents a value lower than the true or maximum adhesion strength due to premature failure resulting from non-uniform stress distribution in the Pin-Coating interface. However, the accuracy (*i.e.* the closeness of measured value to the true adhesion strength) of the measured value increases with the increasing coating thickness, since the higher the coating thickness the lesser the non-uniformity in stress distribution. Zone "B" represents the region with measured values close to maximum or true adhesion strength. The true adhesion strength of the thinner coatings can be predicted by extrapolating the linear trendline from Zone "B" (see Figure 10), as proposed by [42,43]. For better prediction of true adhesion strength (by extrapolating method) for thinner coating, it is crucial to identify the transition coating thickness with maximum measured adhesion strength value, for which

additional data points with smaller intervals in coating thickness are required. It is important to note that the Zone “A” and Zone “B” is categorised based on the validity or accurateness of adhesion strength values measured using the Collar-Pin Pull-off Test. The categorisation in this study is not based on failure mechanisms as in [42,43] since the failure mechanisms reported for thermal spray coatings were not comparable with CS Ti-64 coatings.

The Collar-Pin Pull-off Test offers significant benefit compared to the standard ASTM C633 approach as it allows measurement of adhesion strength beyond that of conventional adhesives (70-90 MPa). However, it is recommended that when reporting adhesion strength values for coating thicknesses that fall under Zone A, data should be recorded with a ‘greater than or equal to’ symbol (\geq) before the value to indicate that the measured value is lower than true adhesion strength. Moreover, for Ti-64/Ti-64 coating-substrate assemblies, the proposed test method should not be used to assess thinner coatings (particularly <1.7 mm) owing to very high non-uniformity in stress distribution reaching negative values towards the Pin centre and therefore the likelihood of cohesive or mixed-mode failure. For Zone B, the measured value should be a near-maximum or the true adhesion strength.

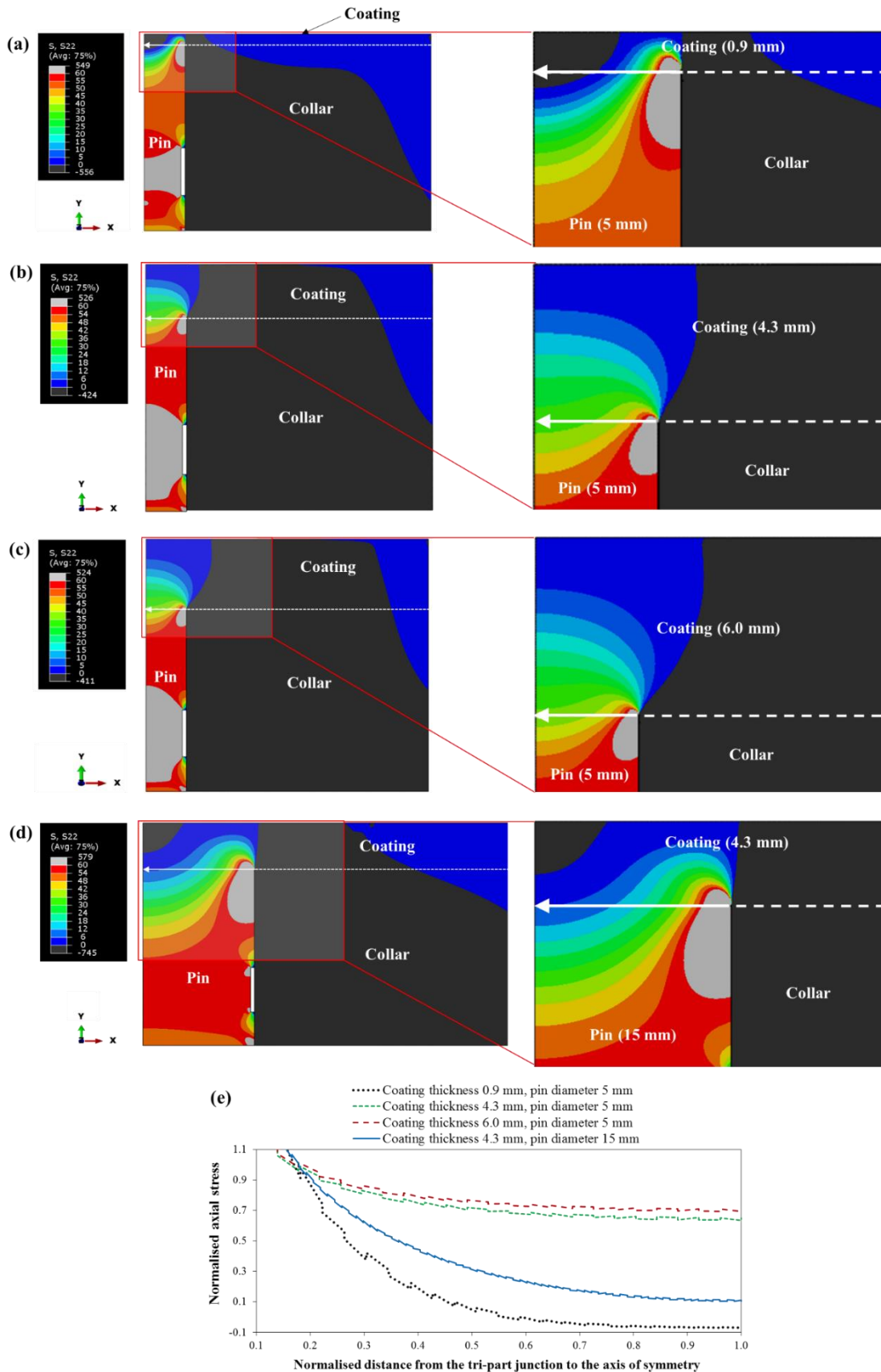


Figure 9: Axial stress contour plots under a nominal applied axial stress of 52 MPa for the models with a 5 mm diameter Pin for coatings thicknesses (a) 0.9 mm, (b) 4.3 mm, and (c) 6.0 mm, respectively; (d) a 15 mm diameter Pin with coating thickness 4.3 mm; (e) comparison of normalised stress (actual stress divided by nominal applied stress) versus normalised distance (distance from Collar-Pin-Coating junction to Pin centre line divided by the Pin radius) for a-d. For the ease of understanding, actual stress vs. distance from the tri-part junction is presented in the Appendix A3 (Figure A3).

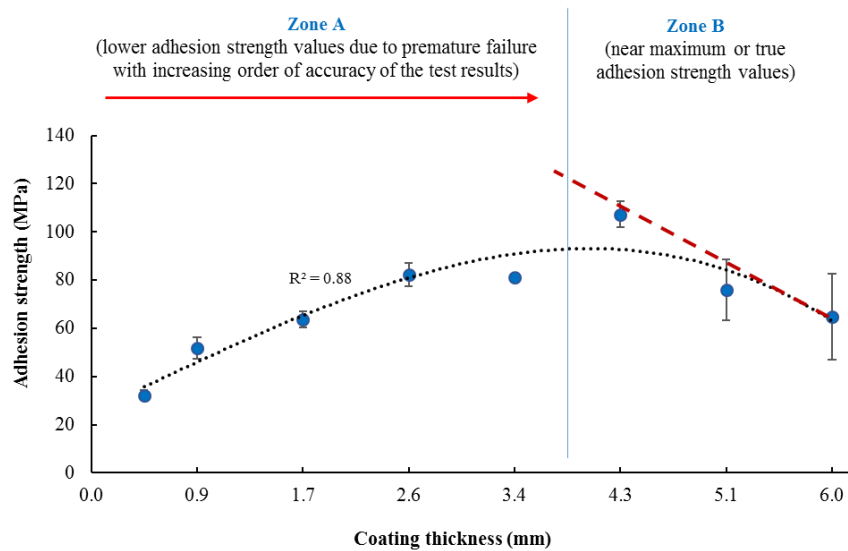


Figure 10: Adhesion strength vs coating thickness in terms of accurateness (closeness to true adhesion strength) of the measured values using the proposed test method, and showing a way of predicting true adhesion strength for thinner coating (Zone A) by extrapolating the linear trendline [42,43] from the region of true adhesion strength (Zone B).

4 Conclusions

An adhesive-free test method referred as modified Collar-Pin Pull-off Test was developed (based on Sharivker's (1967) original design) aiming at overcoming the limitations of existing test methods, for evaluating coating-substrate adhesion strength of high strength coatings such as CS Ti-64. A parametric study was performed on the coating-substrate adhesion strength in terms of the influence of coating thickness, scanning speed, toolpath pattern, track spacing, and substrate surface preparation. Finite element analysis was performed to understand the stress distribution during the pull-off loading for the proposed adhesive-free test method. All the specimens were deposited using N₂ as a process gas at 1100 °C and 5 MPa. The conclusions from this study can be summarised as follows:

1. The proposed adhesive-free test method was found to be capable of measuring coating-substrate adhesion strength beyond the upper limit (70-90 MPa) of conventional adhesive based methods such as ASTM C633. In the case of CS Ti-64, the highest value of adhesion strength was measured as 122 ± 2.8 MPa for the ground substrate with a 320 grit paper.
2. Computational modelling of the modified Collar-Pin Pull-off Test design showed non-uniform stress distribution at the test area (Pin-Coating interface), which may lead to premature failure resulting in a lower adhesion strength (lower than the true strength). This effect could be more significant for thinner coatings with lower stiffness or considerably larger Pin diameter comparing to the coating thickness. The finite element analysis showed that while the proposed adhesive-free test method allows measurements of coatings with significantly higher adhesion strength, this test underestimates the true adhesion strength particularly for thinner coatings which should be considered when reporting results. The true adhesion strength for thinner coatings can be determined theoretically by extrapolating a linear trendline from the region of thicker coatings possessing true or close to maximum adhesion strength. For CS Ti-64 coatings

deposited on Ti-64 substrates, the proposed test method should not be used to assess thinner coatings (<1.7 mm) due to the likelihood of cohesive or mixed-mode failure.

Acknowledgements

This publication was made possible by the sponsorship and support of the Lloyd's Register Foundation (grant number DB012017COV), which is a charitable organisation that helps to protect life and property by supporting engineering-related education, public engagement and the application of research. Coventry University has also contributed to the PhD studentship (grant number 7486157). This work was partially funded by the Industrial Members of TWI Ltd. through the Core Research Programme (grant number 30643). The authors would like to thank Dr N Smyth, Coventry University for performing Impulse Excitation measurements, and Dr S Paul, TWI for technical support.

References

- [1] N.W. Khun, A.W.Y. Tan, W. Sun, E. Liu, Wear and Corrosion Resistance of Thick Ti-6Al-4V Coating Deposited on Ti-6Al-4V Substrate via High-Pressure Cold Spray, *J. Therm. Spray Technol.* 26 (2017) 1393–1407. doi:10.1007/s11666-017-0588-8.
- [2] R.R. Boyer, An overview on the use of titanium in the aerospace industry, *Mater. Sci. Eng. A.* 213 (1996) 103–114. doi:10.1016/0921-5093(96)10233-1.
- [3] W. Zhuang, Q. Liu, R. Djugum, K. Sharp, Additive Manufacturing for Aircraft Component Repair, in: *Aircr. Airworth. Sustain. Conf. Brisbane*, 2016.
- [4] A.W.Y. Tan, W. Sun, Y.P. Phang, M. Dai, I. Marinescu, Z. Dong, E. Liu, Effects of traverse scanning speed of spray nozzle on the microstructure and mechanical properties of cold-sprayed Ti6Al4V coatings, *J. Therm. Spray Technol.* 26 (2017) 1484–1497. doi:10.1007/s11666-017-0619-5.
- [5] R. Liu, Z. Wang, T. Sparks, F. Liou, J. Newkirk, Aerospace component repair with additive manufacturing, in: *Laser Addit. Manuf.*, Elsevier Ltd, 2017: pp. 361–371. doi:10.1016/B978-0-08-100433-3.00013-0.
- [6] B. Sheerman, C. Spelman, Tripple Win: The Social, Economic and Environmental Case for Remanufacturing, 2014. <http://www.remanufacturing.org.uk/pdf/story/2p650.pdf>.
- [7] D. Boruah, B. Ahmad, T.L. Lee, S. Kabra, A.K. Syed, P. McNutt, M. Doré, X. Zhang, Evaluation of residual stresses induced by cold spraying of Ti-6Al-4V on Ti-6Al-4V substrates, *Surf. Coatings Technol.* 374 (2019) 591–602.
- [8] A. Papyrin, *Cold spray technology*, Elsevier, 2007.
- [9] T. Suhonen, T. Varis, S. Dosta, M. Torrell, J.M. Guilemany, Residual stress development in cold sprayed Al, Cu and Ti coatings, *Acta Mater.* 61 (2013) 6329–6337. doi:10.1016/j.actamat.2013.06.033.
- [10] A.M. Birt, V.K. Champagne, R.D. Sisson, D. Apelian, Microstructural Analysis of Cold-Sprayed Ti-6Al-4V at the Micro- and Nano-Scale, *J. Therm. Spray Technol.* 24 (2015) 1277–1288. doi:10.1007/s11666-015-0288-1.
- [11] A.W.Y. Tan, W. Sun, A. Bhowmik, J.Y. Lek, I. Marinescu, F. Li, N.W. Khun, Z. Dong, E. Liu, Effect of coating thickness on microstructure, mechanical properties and fracture behaviour of cold sprayed Ti6Al4V coatings on Ti6Al4V substrates, *Surf. Coatings Technol.* 349 (2018) 303–317. doi:10.1016/j.surfcoat.2018.05.060.

- [12] J.Y. Lek, A. Bhowmik, A.W.Y. Tan, W. Sun, X. Song, W. Zhai, P.J. Buenconsejo, F. Li, E. Liu, Y.M. Lam, C.B. Boothroyd, Understanding the microstructural evolution of cold sprayed Ti-6Al-4V coatings on Ti-6Al-4V substrates, *Appl. Surf. Sci.* 459 (2018) 492–504. doi:10.1016/j.apsusc.2018.07.175.
- [13] M.V. Vidaller, A. List, F. Gaertner, T. Klassen, S. Dosta, J.M. Guilemany, Single Impact Bonding of Cold Sprayed Ti-6Al-4V Powders on Different Substrates, *J. Therm. Spray Technol.* 24 (2015) 644–658. doi:10.1007/s11666-014-0200-4.
- [14] N.W. Khun, A.W.Y. Tan, K.J.W. Bi, E. Liu, Effects of working gas on wear and corrosion resistances of cold sprayed Ti-6Al-4V coatings, *Surf. Coatings Technol.* 302 (2016) 1–12. doi:10.1016/j.surfcoat.2016.05.052.
- [15] V.N.V. Munagala, T.B. Torgerson, T.W. Scharf, R.R. Chromik, High temperature friction and wear behavior of cold-sprayed Ti6Al4V and Ti6Al4V-TiC composite coatings, *Wear.* 426–427 (2019) 357–369. doi:10.1016/j.wear.2018.11.032.
- [16] P. Vo, E. Irissou, J.G. Legoux, S. Yue, Mechanical and microstructural characterization of cold-sprayed Ti-6Al-4V after heat treatment, *J. Therm. Spray Technol.* 22 (2013) 954–964. doi:10.1007/s11666-013-9945-4.
- [17] C. Chen, Y. Xie, X. Yan, S. Yin, R. Huang, R. Zhao, J. Wang, Z. Ren, M. Liu, H. Liao, Effect of hot isostatic pressing (HIP) on microstructure and mechanical properties of Ti6Al4V alloy fabricated by cold spray additive manufacturing, *Addit. Manuf.* (2019) 1–31. doi:10.1016/j.addma.2019.03.028.
- [18] N.W. Khun, A.W.Y. Tan, W. Sun, E. Liu, Effect of Heat Treatment Temperature on Microstructure and Mechanical and Tribological Properties of Cold Sprayed Ti-6Al-4V Coatings, *Tribol. Trans.* 60 (2017) 1033–1042. doi:10.1080/10402004.2016.1244584.
- [19] V.S. Bhattiprolu, K.W. Johnson, O.C. Ozdemir, G.A. Crawford, Influence of feedstock powder and cold spray processing parameters on microstructure and mechanical properties of Ti-6Al-4V cold spray depositions, *Surf. Coatings Technol.* 335 (2018) 1–12. doi:10.1016/j.surfcoat.2017.12.014.
- [20] D. Goldbaum, J.M. Shockley, R.R. Chromik, A. Rezaeian, S. Yue, J.G. Legoux, E. Irissou, The effect of deposition conditions on adhesion strength of Ti and Ti6Al4V cold spray splats, *J. Therm. Spray Technol.* 21 (2012) 288–303. doi:10.1007/s11666-011-9720-3.
- [21] A. Tan, J. Lek, W. Sun, A. Bhowmik, I. Marinescu, X. Song, W. Zhai, F. Li, Z. Dong, C. Boothroyd, E. Liu, Influence of Particle Velocity When Propelled Using N₂ or N₂-He Mixed Gas on the Properties of Cold-Sprayed Ti6Al4V Coatings, *Coatings.* 8 (2018) 327. doi:10.3390/coatings8090327.
- [22] P. Sirvent, M.A. Garrido, C.J. Múñez, P. Poza, A. Cazacu, R. Barnett, H.L. De Villiers, Effect of powder geometry on the mechanical performance of cold sprayed Ti-6Al-4V coatings, in: *XXX Int. Conf. Surf. Modif. Technol.*, Milan, Italy, 2016: pp. 1–8.
- [23] V.N.V. Munagala, V. Akinyi, P. Vo, R.R. Chromik, Influence of Powder Morphology and Microstructure on the Cold Spray and Mechanical Properties of Ti6Al4V Coatings, *J. Therm. Spray Technol.* 27 (2018) 827–842. doi:10.1007/s11666-018-0729-8.
- [24] V.N.V. Munagala, S.I. Imbriglio, R.R. Chromik, The influence of powder properties on the adhesion strength and microstructural evolution of cold sprayed Ti6Al4V single splats, *Mater. Lett.* 244 (2019) 58–61. doi:10.1016/j.matlet.2019.02.028.
- [25] V. Satish, B. Kyle, W.J. Grant, Influence of Powder Microstructure on the Microstructural Evolution of As-Sprayed and Heat Treated Cold-Sprayed Ti-6Al-4V Coatings, *J. Therm. Spray Technol.* 28 (2019) 174–188. doi:10.1007/s11666-018-0812-1.

- [26] W. Wong, E. Irissou, J.G. Legoux, P. Vo, S. Yue, Powder Processing and Coating Heat Treatment on Cold Sprayed Ti-6Al-4V Alloy, *Mater. Sci. Forum.* 706–709 (2012) 258–263. doi:10.4028/www.scientific.net/MSF.706-709.258.
- [27] H. Aydin, M. Alomair, W. Wong, P. Vo, S. Yue, Cold Sprayability of Mixed Commercial Purity Ti Plus Ti6Al4V Metal Powders, *J. Therm. Spray Technol.* 26 (2017) 360–370. doi:10.1007/s11666-017-0528-7.
- [28] X. Luo, Y. Wei, Y. Wang, C. Li, Microstructure and mechanical property of Ti and Ti6Al4V prepared by an in-situ shot peening assisted cold spraying, *Mater. Des. J.* 85 (2015) 527–533. doi:10.1016/j.matdes.2015.07.015.
- [29] W. Sun, A.W.Y. Tan, N.W. Khun, I. Marinescu, E. Liu, Effect of substrate surface condition on fatigue behavior of cold sprayed Ti6Al4V coatings, *Surf. Coatings Technol.* 320 (2017) 452–457. doi:10.1016/j.surfcoat.2016.11.093.
- [30] ASTM C633-13(2017), Standard Test Method for Adhesion or Cohesion Strength of Thermal Spray Coatings, ASTM Int. (2017). www.astm.org.
- [31] BS EN ISO 14916:2017 - Thermal spraying. Determination of tensile adhesive strength, BSI. (2017).
- [32] S. Costil, Y. Danlos, W. Wong, THE PROTAL ® process applied on Cold Spraying to improve interface adherence and coating cohesion – case of titanium and nickel based alloys NRC Publications Archive (NPArc) Archives des publications du CNRC (NPArc) THE PROTAL ® process applied on Col, NRC CNRC. (2010).
- [33] R. Huang, H. Fukanuma, Study of the influence of particle velocity on adhesive strength of cold spray deposits, *J. Therm. Spray Technol.* 21 (2012) 541–549. doi:10.1007/s11666-011-9707-0.
- [34] R. Huang, W. Ma, H. Fukanuma, Development of ultra-strong adhesive strength coatings using cold spray, *Surf. Coatings Technol.* 258 (2014) 832–841. doi:10.1016/j.surfcoat.2014.07.074.
- [35] E. Irissou, J.-G. Legoux, B. Arsenault, C. Moreau, Investigation of Al-Al₂O₃ Cold Spray Coating Formation and Properties, *J. Therm. Spray Technol.* 16 (2007) 661–668. doi:10.1007/s11666-007-9086-8.
- [36] G. Bae, S. Kumar, S. Yoon, K. Kang, H. Na, H.-J. Kim, C. Lee, Bonding features and associated mechanisms in kinetic sprayed titanium coatings, *Acta Mater.* 57 (2009) 5654–5666. doi:10.1016/j.actamat.2009.07.061.
- [37] C. Lyphout, P. Nysten, L.G. Östergren, Adhesion strength of HVOF sprayed IN718 coatings, *J. Therm. Spray Technol.* 21 (2012) 86–95. doi:10.1007/s11666-011-9689-y.
- [38] B. Robinson, Adhesive-free Bond Strength Test Method for Cold Spray Coatings, Industrial Member Report Prepared for the Industrial Members of TWI Ltd, Cambridge, UK, 2019.
- [39] ASTM D4541 – 17, Standard Test Method for Pull-Off Strength of Coatings Using Portable Adhesion Testers, ASTM Int. (2017). www.astm.org.
- [40] ISO 4624:2016 - Paints and varnishes -- Pull-off test for adhesion, ISO. (2016).
- [41] C.K. Lin, C.C. Berndt, Measurement and analysis of adhesion strength for thermally sprayed coatings, *J. Therm. Spray Technol.* 3 (1994) 75–104. doi:10.1007/BF02649003.
- [42] S.Y. Sharivker, Strength of adhesion of plasma sprayed coatings to the base material, *Sov. Powder Metall. Met. Ceram.* 6 (1967) 483–485. doi:https://doi.org/10.1007/BF00780138.
- [43] B.A.. Lyashenko, V.V.. Rishin, V.G.. Zil'berberg, S.Y. Sharivker, Strength of adhesion between plasma-sprayed coatings and the base metal, *Sov. Powder Metall. Met. Ceram.* 8

- (1969) 331–334. doi:<https://doi.org/10.1007/BF00776085>.
- [44] ASTM C1624 – 05, Standard Test Method for Adhesion Strength and Mechanical Failure Modes of Ceramic Coatings by Quantitative Single Point Scratch Testing, ASM Int. (2015).
- [45] BS ISO 19207:2016 - Thermal spraying. Classification method of adhesive strength by indentation, BSI. (2016).
- [46] ASTM D3167 – 10, Standard Test Method for Floating Roller Peel Resistance of Adhesives, ASTM Int. (2017). www.astm.org.
- [47] ASTM D903 – 98, Standard Test Method for Peel or Stripping Strength of Adhesive Bonds, ASTM Int. (2017). www.astm.org.
- [48] C.H. Boyle, S.A. Meguid, Mechanical performance of integrally bonded copper coatings for the long term disposal of used nuclear fuel, *Nucl. Eng. Des.* 293 (2015) 403–412. doi:10.1016/j.nucengdes.2015.08.011.
- [49] X. Chen, C. Shaw, L. Gelman, K.T. V Grattan, Advances in test and measurement of the interface adhesion and bond strengths in coating-substrate systems , emphasising blister and bulk techniques, *Measurement*. 139 (2019) 387–402. doi:10.1016/j.measurement.2019.03.026.
- [50] D.J. Greving, J.R. Shadley, E.F. Rybicki, D.J. Greving, J.R. Shadley, E.F. Rybicki, Effects of coating thickness and residual stresses on the bond strength of ASTM C633-79 thermal spray coating test specimens, *J. Therm. Spray Technol.* 3 (1994) 371–378. doi:10.1007/BF02658982.
- [51] D. Boruah, X. Zhang, M. Doré, Theoretical prediction of residual stresses induced by cold spray with experimental validation, *Multidiscip. Model. Mater. Struct.* 15 (2019) 599–616. doi:10.1108/MMMS-08-2018-0150.
- [52] ISO - ISO 4288:1996 - Geometrical Product Specifications (GPS) — Surface texture: Profile method — Rules and procedures for the assessment of surface texture, ISO. (1996). <https://www.iso.org/standard/2096.html>.
- [53] B.A. Lyashenko, V. V. Rishin, E.A. Astakhov, S.Y. Sharivker, Investigation of the adhesion strength coatings applied by detonation-gun flame spraying, *Strength Mater.* 4 (1972) 287–290. doi:<https://doi.org/10.1007/BF01528405>.
- [54] H. Lovelock, B. Robinson, Progress Report: Adhesive-free Bond Strength Test for Cold Spray Coatings, in: CSAT, 2017. [https://www.coldsprayteam.com/Lovelock_Final CSAT 2017_Adhesive-free Bond Strength Test Method for Cold Spray Coatings.pdf](https://www.coldsprayteam.com/Lovelock_Final%202017_Adhesive-free%20Bond%20Strength%20Test%20Method%20for%20Cold%20Spray%20Coatings.pdf).
- [55] ASTM E1876 – 15, Standard Test Method for Dynamic Young’s Modulus, Shear Modulus, and Poisson’s Ratio by Impulse Excitation of Vibration, ASTM Int. (2015). www.astm.org.
- [56] V. Champagne, S. Dinavahi, P. Leyman, Prediction of Particle Velocity for the Cold Spray Process (ARL-TR-5683), 2011. <http://oai.dtic.mil/oai/oai?verb=getRecord&metadataPrefix=html&identifier=ADA551777>.
- [57] T. Hussain, Cold spraying of titanium: A review of bonding mechanisms, microstructure and properties, *Key Eng. Mater.* 533 (2012) 53–90. doi:10.4028/www.scientific.net/KEM.533.53.
- [58] R. Singh, S. Schrufer, S. Wilson, J. Gibmeier, R. Vassen, Influence of coating thickness on residual stress and adhesion-strength of cold-sprayed Inconel 718 coatings, *Surf. Coatings Technol.* 350 (2018) 64–73. doi:10.1016/j.surfcoat.2018.06.080.
- [59] L. Berthe, M. Arrigoni, M. Boustie, State-of-the-art laser adhesion test (LASAT), *Nondestruct. Test. Eval.* 26 (2011) 303–317. doi:10.1080/10589759.2011.573550.

Appendix A

A1. Existing test methods for measuring coating adhesion strength

Adhesive-based test methods for determining coating adhesion strength includes: (i) Tensile Adhesion Test (TAT) as per ASTM C633 [30] or BS EN ISO 14916 [31] or modified versions of ASTM C633 [4,11,38], (ii) Portable Adhesion Test (PAT) based on ASTM D4541 [39] or ISO 4624 [40], and (iii) Double Cantilever Beam (DCB) Test [41]. Adhesive-free methods comprises of: (i) Scratch Test as per ASTM C1624 [44], (ii) Interfacial Indentation Test as per BS ISO 19207 [45], (iii) Peel Test as per ASTM D3167 [46] and ASTM D903 [47], (vi) Tie Bar Test [41], (vii) modified ASTM E8 [11,48] or modified ASTM C633 [33,34], and (vii) Laser Shock Adhesion Test (LASAT) [49,59]. Schematics of these test methods are presented in Figure A1.

A2. Effect of process and geometrical variables on the residual stresses

The influence of process and geometrical variables such as- (i) coating thickness (Figure A2a), (ii) scanning speed or individual layer thickness (Figure A2b), and (iii) toolpath pattern (Figure A2b) on residual stresses measured by the Contour method are presented in the Figure A2 from our previous work [7]. Also, see our previous work [51] on a parametric study on residual stresses using an analytical model.

A3. FEA results: Axial stress along the interface

FEA stress analysis results showing axial stress distribution along the Pin-Coating interface versus the distance from the Collar-Pin-Coating junction towards the Pin centre (under the nominal applied stress of 52 MPa) for a 5 mm diameter Pin with three coating thicknesses 0.9, 4.3, and 6.0 mm (Figure A3a), and for a 15 mm diameter Pin with 4.3 m coating thickness (Figure A3b).

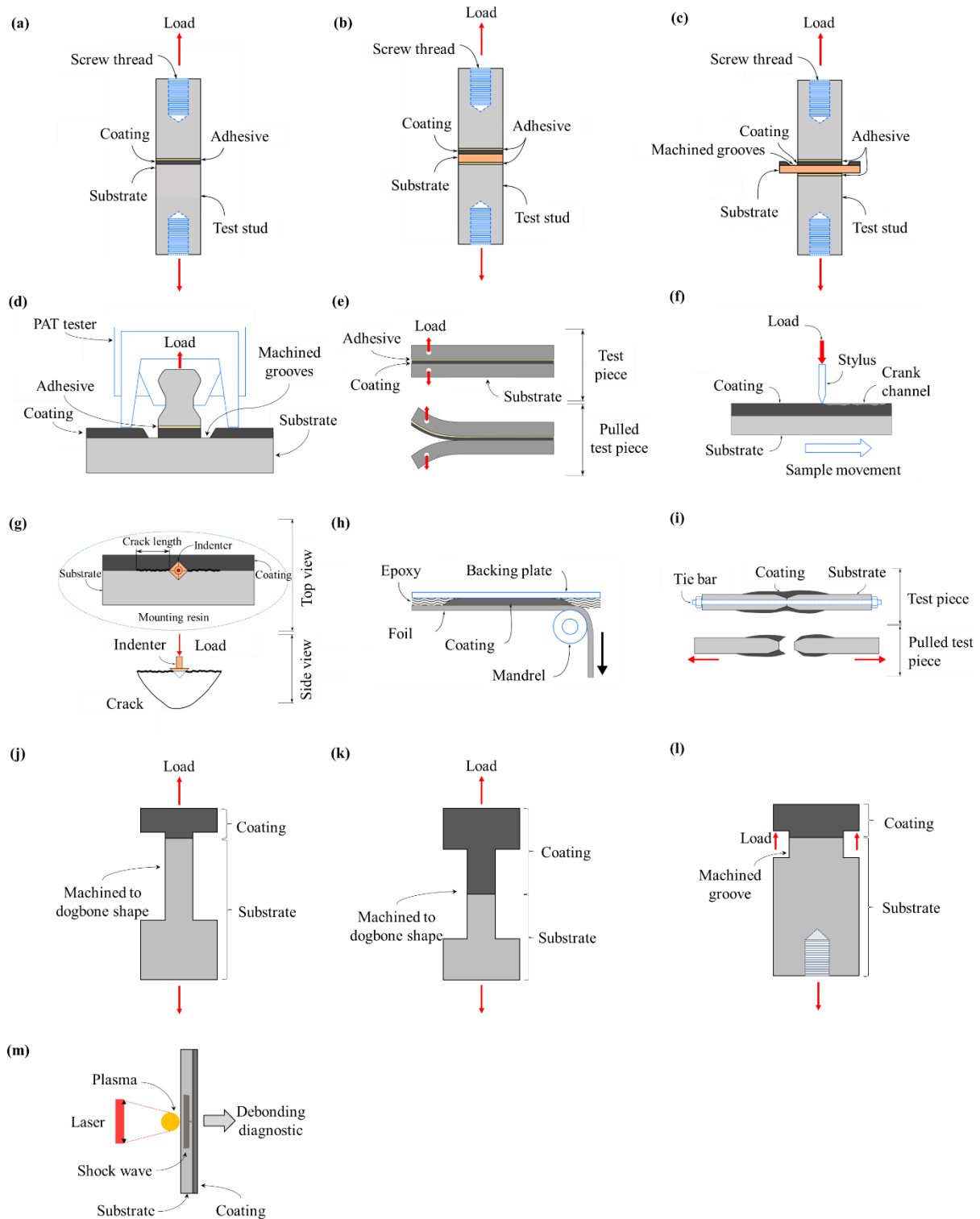


Figure A1: Schematic of various methods for measuring coating-substrate adhesion strength: (a) TAT as per ASTM C633 [30] (b) modified ASTM C633 specimen for round bar substrate having similar diameter as the test stud [4,11], (c) modified ASTM C633 specimen for square substrate or round bar substrate with higher diameter than the test stud [38], (d) PAT as per ASTM D4541 [39], (e) Double Cantilever Beam Test [41], (f) Scratch Test as per ASTM C1624 [44], (g) Interfacial Indentation Test as per BS ISO 19207 [45], (h) Peel test as per ASTM D3167 [46] and ASTM D903 [47], (i) Tie Bar Test [41], (j) Modified ASTM E8 [11], (k) Modified ASTM E8 [48], (l) modified adhesive-free ASTM C633 [33,34], and (m) Laser Shock Adhesion Test (LASAT) [59].

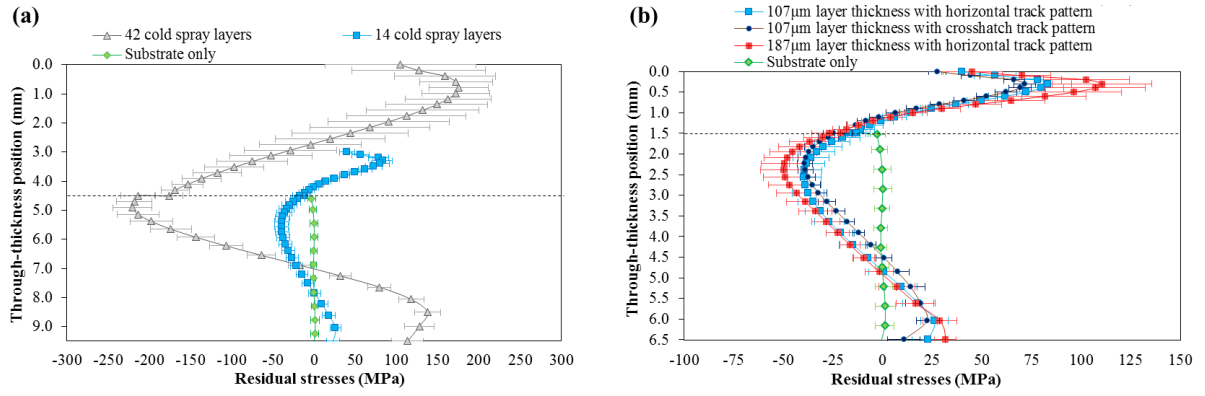


Figure A2: Effect of (a) coating thickness, (b) toolpath pattern (horizontal raster and cross-hatch), and individual layer thickness or scanning speed ($\sim 107 \mu\text{m}$ average layer thickness at 500 mm/s, and $\sim 187 \mu\text{m}$ at 300 mm/s) on residual stresses, measured by the Contour method [7].

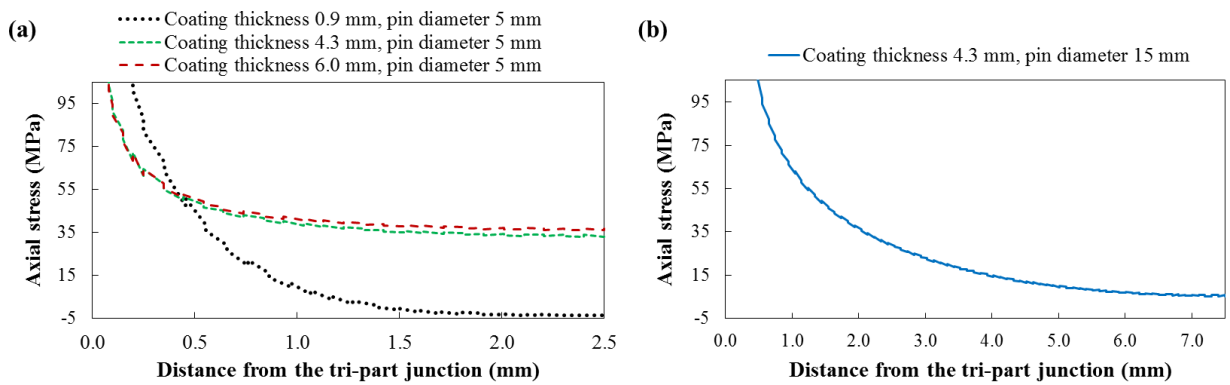


Figure A3: FEA stress analysis results showing axial stress distribution along the interface from the tri-part junction to the Pin centre for (a) 5 mm Pin diameter with 0.9, 4.3, and 6.0 mm thick coatings, (b) 15 mm Pin diameter with coating thickness of 4.3 mm.